Lecture 16: Spatial Pattern Formation by Turing Instability

Physics 221A, Spring 2017
Lectures: Prof. P. H. Diamnod
Notes: Xiang Ji

June 2, 2017

1 Introduction

Turing Instability is a simple mechanism for generating heterogeneous spatial patterns via reaction-diffusion system. Let's consider two coupled scalar fields system:

$$\begin{aligned} \frac{\partial A}{\partial \tau} &= F(A,B) + D_A \nabla^2 A \\ \frac{\partial B}{\partial \tau} &= G(A,B) + D_B \nabla^2 B, \end{aligned} \tag{1}$$

where D_A and D_B are diffusion coefficient of A and B, respective, $F(A,B)$ and $G(A,B)$ characterize the kinetics of chemical reaction, which are generally nonlinear. One example of the kinetic term is the Schnakenberg model for the minimal chemical system exhibiting limit-cycle behavior:

$$\begin{aligned} F(A,B) &= k_1 - k_2 + k_3 A^2 B \\ G(A,B) &= k_4 - k_3 A^2 B, \end{aligned} \tag{2}$$

where $k_i > 0$ are chemical reaction coefficients. Another example is the activator-inhibitor model:

$$\begin{aligned} F(A,B) &= k_1 - k_2 + k_3 A^2/B \\ G(A,B) &= k_4 A^2 - k_5 B, \end{aligned} \tag{3}$$

In the absence of diffusion, A and B tend to have a uniform stationary state. However, Turing pointed out that if $D_A \neq D_B$, it's possible for the system to have an spatially heterogeneous solution. The diffusion term, which in many cases is the stabilizing factor preventing pattern formation, becomes essential to drive pattern formation in this case.

To understand the destabilizing effect of diffusion intuitively, let's consider the following scenario: a population of grasshoppers live on the grass field. When the grasshopper feels hot, it sweat to increase the moisture of the environment. In the hot dry summer, the grass becomes direr and drier, some part of the grass somehow get burned. When our super grasshoppers feel the fire(more than warm), they begin to sweat, which can make the environment so wet that can effectively damp the prorogation of the front of the fire. Assuming that the diffusion coefficient of the fire D_F is much smaller than that of the grasshopper D_G and the grass randomly get burned on the field, we can expect each spot of fire will be surrounded by a bunch of our super grasshoppers and eventually a heterogeneously pattern of fire and grasshoppers will form.

Now, let's consider what's important in this dynamical system. The first one is the interaction. The kinetic term $F(A,B)$ and $G(A,B)$ might characterize the rate of grass get burned, how does the sweat damp the fire and the grasshoppers sweating rate. Second, the diffusion coefficient of fire and grasshoppers, which is essential to *diffusion driven instability*. Combined with the scale of the field(characterize by L), we get two

critical time scale for the spreading of grasshoppers and fire, D_H/L^2 and D_F/L^2, respectively. And third, the boundary condition is also important.

Before starting analyzing, it's useful to rewrite Eqn.1 into dimensionless form. Taking the kinetic term in Eqn.2 as an example. Let:

$$\begin{aligned} &u = A(K_3/K_2)^{1/2},\ v = B(k_3/k_2)^{1/2},\ t^* = D_A t/L^2,\ x^* = x/L, \\ &d = D_B/D_A,\ a = \frac{k_1}{k_2}(\frac{k_3}{k_2})^{1/2}, \\ &b = \frac{k_4}{k_2}(\frac{k_3}{k_2})^{1/2}, \gamma = \frac{L^2 k_2}{D_A}. \end{aligned} \tag{4}$$

we get the following dimensionless form:

$$\begin{aligned} \frac{\partial u}{\partial t} &= \gamma(a - u + u^2 v) + \nabla^2 u = \gamma f(u,v) + \nabla^2 v \\ \frac{\partial v}{\partial t} &= \gamma(b - u^2 v) + d\nabla^2 v = \gamma g(u,v) + d\nabla^2 u, \end{aligned} \tag{5}$$

Note that here $\gamma \sim L^2$.

2 Linear Stability Analysis

We define the system with zero flux boundary condition:

$$\begin{cases} \frac{\partial u}{\partial t} = \gamma f(u,v) + \nabla^2 v \\ \frac{\partial v}{\partial t} = \gamma g(u,v) + d\nabla^2 u \\ \hat{n}\cdot\nabla u = \hat{n}\cdot\nabla v = 0 \ \textit{on all the boundary} \\ u(r, t=0), v(r, t=0) \ \textit{given} \end{cases} \tag{6}$$

2.1 Linear Stability Without Diffusion

We assume that without diffusion, the system has a linearly stable spatial-homogeneous solution (v_0, u_0). ThE stability of the system can be examined by a small perturbation:

$$\begin{aligned} u &= u_0 + \tilde{u} \\ v &= v_0 + \tilde{v}, \end{aligned} \tag{7}$$

and Eqn. 6 becomes:

$$\frac{d}{dt}\begin{pmatrix}\tilde{u}\\ \tilde{v}\end{pmatrix} = \gamma \begin{pmatrix} \frac{\partial f}{\partial u} & \frac{\partial f}{\partial v} \\ \frac{\partial g}{\partial u} & \frac{\partial g}{\partial v} \end{pmatrix}\Bigg|_{(u_0,v_0)} \begin{pmatrix}\tilde{u}\\ \tilde{v}\end{pmatrix} \equiv A \begin{pmatrix}\tilde{u}\\ \tilde{v}\end{pmatrix} \tag{8}$$

The sign of the eigenvalue of A indicate the stability of the system:

$$\begin{vmatrix} \gamma\frac{\partial f}{\partial u} - \lambda & \gamma\frac{\partial f}{\partial v} \\ \gamma\frac{\partial g}{\partial u} & \gamma\frac{\partial g}{\partial v} - \lambda \end{vmatrix} = 0 \tag{9}$$

thus:

$$\lambda = \frac{\gamma}{2}[tr(A) \pm \sqrt{tr(A) - 4\det(A)}] \tag{10}$$

To have a stable system, λ should be negative, which requires $tr(A) < 0$ and $\det(A) > 0$ and thus impose constrains on the properties of the kinetic function $f(u,v)$ and $g(u,v)$. In the following analysis, we always assume that the system is linearly stable in the absence of diffusion.

2.2 Diffusion driven instability

Now let's consider the whole problem. Define $\mathbf{w} = (\tilde{u}, \tilde{v})^T$, Eqn. 6 becomes:

$$\frac{\partial \mathbf{w}}{\partial t} = \mathbf{D}\nabla^2\mathbf{w} + \gamma A\mathbf{w},\ D = \begin{pmatrix} 1 & 0 \\ 0 & d \end{pmatrix} \tag{11}$$

To solve this problem, we take the Fourier transformation of the $\mathbf{w}$:

$$\mathbf{w} = \sum_k c_k e^{\lambda t}\mathbf{w_k}(\mathbf{r}) \tag{12}$$

For each mode of the time-independent component, $\mathbf{w}_k(r)$ satisfies the following equations with the same boundary condition as the original equation Eqn.6:

$$\begin{aligned} &\nabla^2 W + k^2 W = 0 \\ &(\mathbf{n}\cdot\nabla)\mathbf{W} = 0 \textit{ on all the boundary} \end{aligned} \tag{13}$$

The possible value of k in Eqn.13 is determined by the boundary condition. For example, if the system is one dimensional $0 \le x \le a$, we have $\mathbf{w} \propto \cos(n\pi x/a)$, where n is an integer and $k = n\pi/a$. If $\mathbf{w}$ vanishes on the boundary, then $w \propto \sin(n\pi x/a)$.

Substituting Eqn.12 into Eqn.11, we have:

$$\lambda\mathbf{w} = \gamma A\mathbf{w} + D\nabla^2\mathbf{w} \tag{14}$$

To find the eigenvalue:

$$\begin{vmatrix} \gamma f_u - k^2 - \lambda & \gamma f_v \\ \gamma g_u & \gamma g_v - k^2 d - \lambda \end{vmatrix} = 0, \tag{15}$$

thus:

$$2\lambda = [\gamma tr(A) - k^2(d+1)] \pm \sqrt{[\gamma tr(A) - k^2(d+1)]^2 - 4h(k^2)}, \tag{16}$$

where

$$h(k^2) = \gamma \det(A) - \gamma k^2(g_v + df_u) + dk^4 \tag{17}$$

To have instability, at least one eigenvalue λ should be positive. Note that $[\gamma tr(A) - k^2(d+1)]$ is negative-definite, Eqn. 16 can be written as:

$$2\lambda = -|\gamma tr(A) - k^2(d+1)|[1 \pm \sqrt{1 - \frac{h(k^2)}{[\gamma tr(A) - k^2(d+1)]^2}}] \tag{18}$$

For $d = 1$, recall that $tr(A) < 0$ and thus $h(k^2)$ is positive-definite. As a result, both of the eigenvalues are negative and thus the system is linearly stable, which confirms that the difference between diffusion coefficient is essential for the diffusion driven instability. For $d \neq 1$, let's look at the minimum of $h(k^2)$:

$$\frac{dh}{dk^2} = -\gamma(g_v + df_u) + 2dk^2 = 0, \tag{19}$$

which gives the wavenumber that minimize $h(k^2)$:

$$h_{min} = \gamma^2 \det(A) - \frac{\gamma^2(g_v + df_u)^2}{4d},\ k_m^2 = \frac{\gamma(g_v + df_u)}{2d}. \tag{20}$$

Here, k_m characterizes the scale of the pattern. Linear instability requires h_{min} to be negative. The critical diffusion coefficient ratio d_c is given by:

$$d^2 f_u^2 + 2(2g_u f_v - f_u g_v)d + g_v^2 = 0 \tag{21}$$

$$d_c = \frac{f_u g_v - 2g_u f_v \pm \sqrt{g_u^2 f_v^2 - f_u f_v g_u g_v}}{f_u^2} \tag{22}$$

And the corresponding critical wavenumber is:

$$k_c^2 = \frac{\gamma(g_v + df_u)}{2d_c} = \gamma\sqrt{\frac{\det(A)}{d_c}}, \tag{23}$$

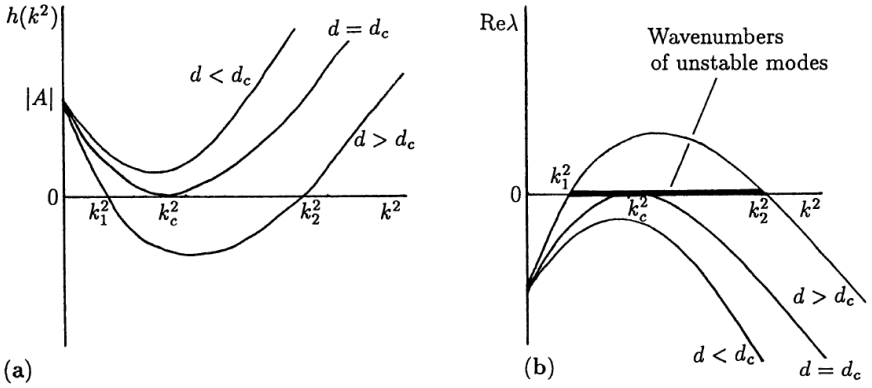

Figure 1: (a) When diffusion coefficient ratio d becomes larger than d_c, there exist a range of k^2 such that $h(k^2) < 0$, which results in the positive real part of the eigenvalue λ, as shown in (b)[1]

As the diffusion coefficient ratio d increase, the value of $h(k^2)$ decreases. A typical $h(k^2)$ is shown in Fig.1. If $d < d_c$, then $h(k^2) = 0$ has two solutions:

$$k_{1,2}^2 = \frac{\gamma(g_v + df_u) \pm \sqrt{\gamma^2(g_v + df_u)^2 - 4d\gamma\det(A)}}{2d} \tag{24}$$

When $h(k^2)$ becomes negative, one of the eigenvalues in Eqn.18 is positive for $k_1^2 < k^2 < k_2^2$, indicating that the magnitude of these modes $\mathbf{w}_k(r)$ increase exponentially over time and form a heterogeneous spatial pattern.

3 Analysis of Patterns

One of the generic questions that one might ask is how does the structure of the pattern depends on the size and the geometry of the system. As shown in Fig. 1-(b), the critical mode k_c gives the largest positive real part of the eigenvalue λ and thus grows fastest. However, the possible value of k is determined by the boundary condition.

3.1 Single Unstable Mode

Considering the following example:

$$\begin{aligned} &\frac{d^2u}{dx^2} + \gamma f(u,v) = 0 \\ &d\frac{d^2v}{dx^2} + \gamma g(u,v) = 0 \\ &\frac{du}{dx} = 0, \ x = 0, L \\ &\frac{dv}{dx} = 0, \ x = 0, L \end{aligned} \tag{25}$$

The spatial heterogeneity can be characterize by the heterogeneity function:

$$H = \int_0^L (\frac{du}{dx})^2 + (\frac{dv}{dx})^2 dx \tag{26}$$

Since:

$$\int_0^L (\frac{du}{dx})^2 dx = u\frac{du}{dx}|_0^a - \int_0^L u\frac{d^2u}{dx^2}dx = \int_0^L \gamma u f(u,v)dx, \tag{27}$$

we get:

$$H = \frac{\gamma}{d}\int_0^L [duf(u_v) + vg(u,v)]dx \tag{28}$$

The heterogeneity function has the same form as the energy of the interface growth model. For homogeneous solution, $u_x = v_x = 0$ and thus $H = 0$. For heterogeneous solution, we have positive $H \sim \gamma/d \sim L^2/D_B \sim L^2$: heterogeneity increases as the square of the box size(for 1 dimensional system). According to Eqn.26, the heterogeneity function is an extensive quantity that is proportional to the size of the system. However, in addition to integrating the same mode over a larger system, the number of modes also increases and thus further increases the complexity of patterns and the value of the heterogeneity function. So, how does the size and macroscopic geometry of the system determine the spatial structure of the pattern?

As we have discussed in Eqn.13, the possible value of k is determined by the boundary condition. For **finite** size system with zero-flux boundary condition, the possible value of the spatial wavenumber k is quantized.

$$k_n = \frac{n\pi}{L}, \tag{29}$$

and the number of unstable modes between k_1 and k_2 (Fig.1) is limited.

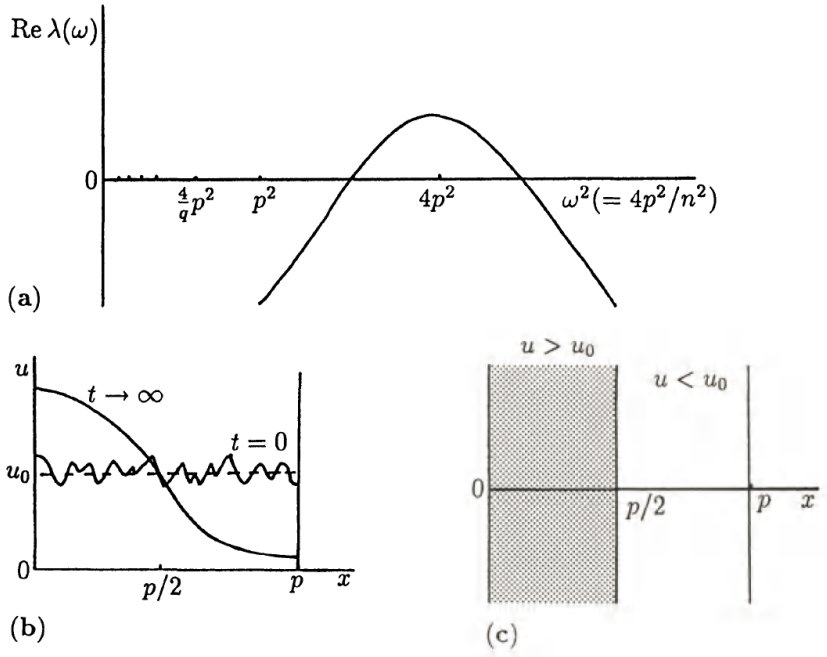

Figure 2: (a) Only one possible wavenumber gives positive real part of the eigenvalue. Here, p is the size of the system(denoted as L above) and ω is the spatial wavelength, which equals $2p$ in this case.(b) Time evolution of mode $n = 1$ in the 1D system in $[0, p]$. (c) Steady heterogeneous pattern [1]

Suppose that only $n = 1$ mode is unstable, as shown in 2-(a). The solution of u can be written in the following form:

$$u(x,t) \sim u_0 + \epsilon \exp(\lambda \frac{\pi^2}{L^2} t) \cos(\frac{\pi x}{L}) \tag{30}$$

Note that we are doing linear stability analysis. With positive eigenvalue, the unstable mode increases exponentially as the system evolve. However, as the amplitude of mode increase, the linear approximation will eventually break down and typically the amplitude will be bound by the nonlinear terms. Here, we consider a system starting from homogeneous state $u(x, t = 0) = const.$ with a small amplitude(ϵ) of mode $n = 1$. As the first order approximation, the temporal evolution of u is shown in Fig.2-(b). By looking at the area with u larger than a threshold u_0, we get a heterogeneous pattern in space (Fig.2-(c)).

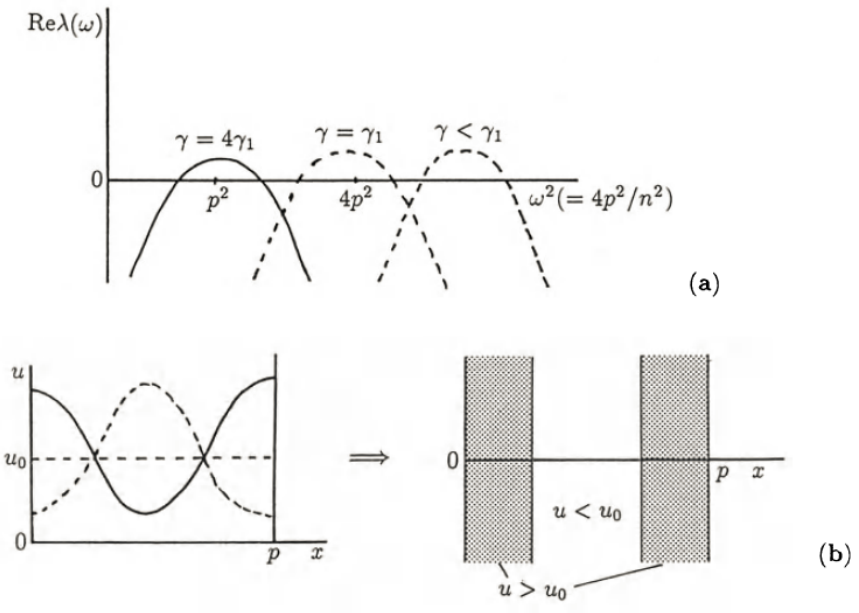

Figure 3: (a) Changing the size of the system shift the dispersion relation of $Re(\lambda(\omega))$. (b) $n = 2$ is the only unstable mode

Now, we have only one unstable mode for the given parameters. If we decrease the size of the system, the curve of $Re(\lambda(\omega))$ will shift to the right and as a result, no unstable mode exist. In contract, if we increase the size of the system by the factor of 2, $n = 1$ mode becomes stable while $n = 2$ mode become the only unstable mode.

3.2 Multiple Unstable Modes

Similarly, for 2D system, the simplest solution is :

$$\mathbf{w}(x,y,t) \sim \sum_{n,m} C_{n,m} \exp(\lambda(k^2)t) \cos(\frac{n\pi x}{p}) \cos(\frac{m\pi y}{q}),\ k^2 = \pi^2(\frac{n^2}{p^2} + \frac{m^2}{q^2}) \tag{31}$$

By changing the parameters of the system, different patterns can be formed,as shown in Fig.4.

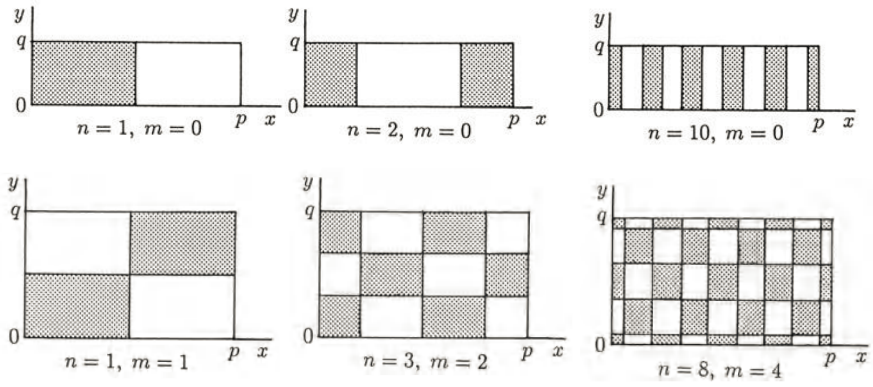

Figure 4: Spatial patterns from by different unstable modes

For system with less simple geometry, the solution to the Helmholtz equation becomes complicated.

$$\nabla^2\psi + k^2\psi = 0,\ (\mathbf{n}\cdot\nabla)\psi = 0\ for\ \mathbf{r} \in \partial B \tag{32}$$

However, for system with certain symmetry, such as square, hexagonal and rhombic, the analytical elementary solutions exist. These solutions form patterns that can tesselate the plane and exhibit the symmetry of the system. For example:

(a) Hexagonal symmetry(Fig. 5-(a)):

$$\psi(x,y) = \frac{\cos k(\frac{\sqrt{3}y}{2} + \frac{x}{2}) + \cos k(\frac{\sqrt{3}y}{2} - \frac{x}{2}) + \cos kx}{3} \tag{33}$$

(b) Square symmetry(Fig. 5-(b)):

$$\psi(x,y) = \frac{\cos kx + \cos ky}{2} \tag{34}$$

(c) Rhombus symmetry(Fig. 5-(c)):

$$\psi(x,y) = \frac{\cos kx + \cos[k(x\cos\phi + y\cos\phi)]}{2}, \tag{35}$$

where ϕ is the rhombus angle.

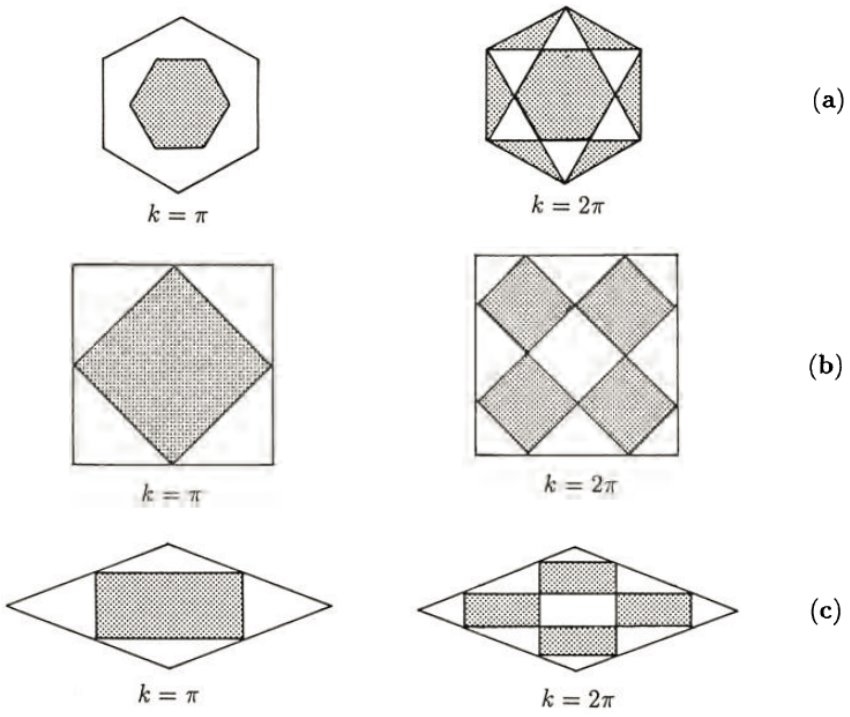

Figure 5: Patterns in systems of different shape[1]

4 Application: Animals Coat Patterns

An interesting application of Turing instability is to explain the animals coat pattern formation. For example, why do most of the cats have ringed tails? What's the origin of zebra's scapular stripes? The answer lies in the morphogenesis of the embryo. During the development of embryo, part of the totipotent cells differentiate into melanoblast and migrate over the surface of the embryo. Then they become melanocytes, which lies in the basal layer of the epidermis. These melanocytes further differentiate into pigment cell and produce melanin, which gives the hair colors. Moreover, it's widely accepted that the synthesis of melanin depends on the presence of a chemical that hasn't been identified yet. In this scenario, cells migrate on the epidermis, interact with the chemical. The diffusion coefficient of the cell is much smaller than the chemical's. Thus, the cells and the chemical form a classical 2 fields reaction-diffusion model, as we have discussed above.

A set of differential equations can be set up by considering detailed mechanism of the process mentioned above. However, very often, analytical solution is inaccessible and thus numerical computation is needed. Before we jump to the numerical results, let's consider the processes qualitatively.

The size and geometry of the system limits the possible mode of patterns. Consider the long-thin tail of cat. It can be modeled as a tapping cylinder of length s and radius $r(z)$, where $z = 0$ corresponds to the bottom of the tail and $z = s$ corresponds the end. By long-thin tail, we assume that $r << s$ With zero-flux boundary condition and periodic boundary condition(natural boundary condition), we expect a solution in the following form:

$$\begin{aligned} &\sum_{n,m} c_{n,m} \exp(\lambda(k^2)t) \cos(n\theta) \cos(\frac{m\pi z}{s}) \\ &k^2 = \frac{n^2}{r^2} + \frac{m^2\pi^2}{s^2} \end{aligned} \tag{36}$$

Since r is relatively small, the number of unstable modes is small and the number decrease as the tail

tapping to the end. In contract, s is relatively large and allow more unstable modes. Longer tail allows more sophisticated patterns. As a result, the fat end of the tail exhibits dot patterns. As r become smaller, mode of lower wavenumber becomes dominant and rings appears. Several numerical solutions are obtained for different parameters and the real patterns on tail are also shown in Fig.6, which are consistent with our discussion.

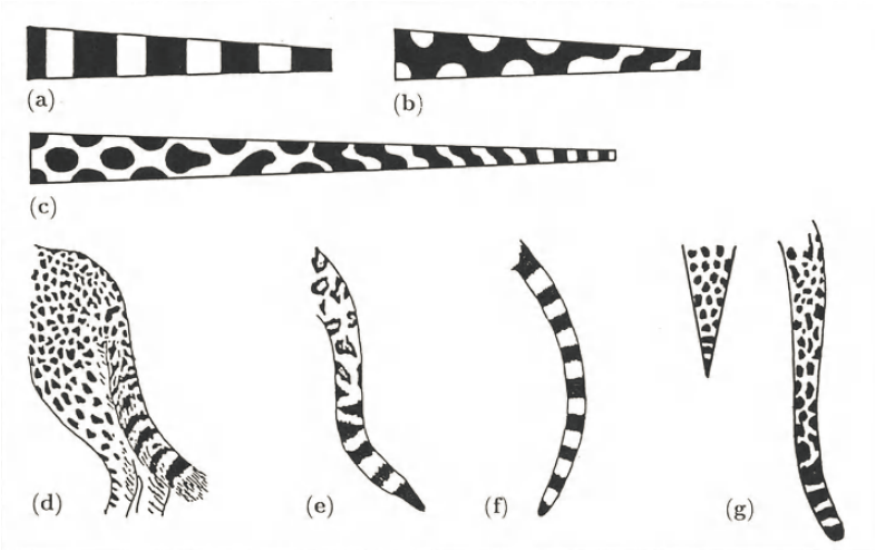

Figure 6: (a)scale factor $\gamma = 9$ (b) scale factor $\gamma = 15$ (c) scale factor $\gamma = 25$, longer domain. (d-g) typical tails[1]

Similar argument can be applied to the zebra patterns. The body and legs can be modeled as cylinders and thus rings appears on the body and the legs. The stripes on body are orthogonal to the legs'. When this two field forms a juncture, the scapular stripes appears(Fig.7)

Figure 7: (a) Typical zebra foreleg stripes (b) predicted pattern by reaction-diffusion equation[1]

5 References

[1]James D. Murray, Mathematical Biology. Springer-Verlag Berlin 2003